RSC Advances

PAPER

View Article Online
View Journal | View Issue

Cite this: *RSC Adv.*, 2020, **10**, 42164

Preferential N–H···:C⩤ hydrogen bonding involving ditopic *NH*-containing systems and *N*-heterocyclic carbenes†

Zacharias J. Kinney, [a] Arnold L. Rheingold[b] and John D. Protasiewicz *[a]

Received 5th October 2020
Accepted 5th November 2020

DOI: 10.1039/d0ra08490e

rsc.li/rsc-advances

Hydrogen bonding plays a critical role in maintaining order and structure in complex biological and synthetic systems. *N*-heterocyclic carbenes (NHCs) represent one of the most versatile tools in the synthetic chemistry toolbox, yet their potential as neutral carbon hydrogen bond acceptors remains underexplored. This report investigates this capability in a strategic manner, wherein carbene-based hydrogen bonding can be assessed by use of ditopic *NH*-containing molecules. N–H bonds are unique as there are three established reaction modes with carbenes: non-traditional hydrogen bonding adducts (X–H···C⩤), salts arising from proton transfer ([H–C⩤]$^+$[X]$^-$), or amines from insertion of the carbene into the N–H bond. Yet, there are no established rules to predict product distributions or the strength of these associations. Here we seek to correlate the hydrogen bond strength of symmetric and asymmetric ditopic secondary amines with 1,3-bis(2,6-diisopropylphenyl)imidazol-2-ylidene (**IPr**, a representative NHC). In symmetric and asymmetric ditopic amine adducts both the solid-state (hydrogen bond lengths, NHC interior angles) and solution-state (^{1}H $\Delta\delta$ of *NH* signals, ^{13}C signals of carbenic carbon) can be related to the pK_a of the parent amine.

Introduction

Hydrogen bonding interactions play a vital role throughout nature and are central to our understanding of complex biological systems.[1] The biological examples of such systems are incalculable, but prominent examples such as DNA, RNA, and enzymatic processes deserve mention.[2–4] Non-biological examples are equally diverse, ranging from controlling the reactivity of small molecules,[5] being central to the unique properties of water,[6,7] to being a key mechanism for generating complex folded structures.[8,9] While the role of hydrogen bonding in complex systems is indisputable, the development of methods to predict and assess the strengths of these interactions are vital to rationally designing novel systems.[10,11]

Hydrogen bond adducts X–H···A involve three-center four-electron bonds formed by interaction of lone pair electrons on a hydrogen bond acceptor (A) with a σ* orbital of a hydrogen bond donor (X–H).[12] In traditional hydrogen bonding, X is an electronegative atom (such as N, O, S, or F) which sufficiently polarizes the X–H bond leading to a reduction of the σ* orbitals energy; and A is generally an electronegative atom (N, O, or halogens) having accessible lone pair electrons.[12–14] Non-traditional hydrogen bonds involving carbon centers are known but relatively rare, with association strengths that are generally weaker than conventional hydrogen bonds.[15] Most often these non-traditional species are mediated *via* formally charged carbon centers (such as isonitriles and carbanions) as the hydrogen bond acceptor.[16,17]

Since the first isolation of singlet carbenes their proliferation to all corners of chemistry are readily apparent.[18–22] Though a variety of singlet carbenes are now synthetically accessible,[23,24] *N*-heterocyclic carbenes (NHCs) based on an imidazole core remain one of the most well-studied and utilized class of carbenes.[21,22,25–27] Shortly after the discovery of isolable NHCs, it was postulated that these compounds could serve as strong hydrogen bond acceptors: with their divalent carbon bearing a lone pair (σ-donor) to interact with a myriad of Brønsted acid X–H species.[28,29] Arduengo described the first example of a carbene-centered hydrogen bond between 1,3-bis(2,4,6-trimethylphenyl)imidazol-2-ium hexafluorophosphate and 1,3-bis(2,4,6-trimethylphenyl)imidazol-2-ylidene (IMes).[30] Clyburne and Davidson later expanded these findings to amine-based non-traditional hydrogen bonding between diphenylamine (**DPA**) and IMes (DPA···IMes, Fig. 1a), showing these species can be structurally authenticated.[31] Movassaghi and Schmidt also identified a MeOH···IMes adduct in their efforts to catalyze

[a]*Department of Chemistry, Case Western Reserve University, Cleveland, Ohio 44106, USA. E-mail: protasiewicz@case.edu*

[b]*Department of Chemistry and Biochemistry, University of California, La Jolla, San Diego, California 92093, USA*

† Electronic supplementary information (ESI) available: Experimental procedures, supplemental figures and analysis, NMR spectra, and crystallographic results. CCDC 2011390, 2011391 and 2011392. For ESI and crystallographic data in CIF or other electronic format see DOI: 10.1039/d0ra08490e

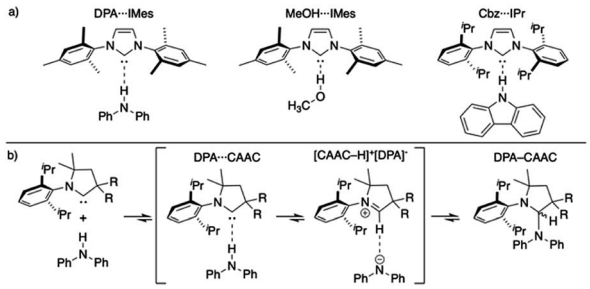

Fig. 1 (a) Representative authenticated X–H···:C< systems;[31–33] (b) general reaction progression elucidated by Bertrand of CAAC inserting into a N–H bond.[34]

amidation reactions with carbenes, authenticating the adduct both in solid- and solution-state (Fig. 1a).[32]

In addition to these reports, other computational[35–39] and experimental[33,40–50] studies on non-traditional X–H···:C< hydrogen bonding have emerged (:C< is neutral carbene species). The balance between non-traditional hydrogen bonding and proton transfer relies on the weak nucleophilicity but high Lewis basicity of NHCs, which can be further modulated *via* variation of the substituents on the imidazole-core.[51,52] Comparison of the available solid-state structures of X–H···:C< hydrogen bonding reveal significant differences can occur. An example of this can be realized in comparing the hydrogen bond lengths (H···:C< distance) in secondary amine-based adducts of carbazole (Cbz) and **DPA** with common NHCs 1,3-bis(2,6-diisopropylphenyl)imidazol-2-ylidene (IPr) and IMes. The hydrogen bond lengths of Cbz···IPr (2.07(3) Å)[33] and DPA···IMes (2.30(2) Å)[31] suggest a stronger interaction for the carbazole *NH* than for the **DPA** *NH* when employing similar NHCs.[53] The interior N–C–N angles of the imidazole-2-ylidene units are slightly distorted as well, where Cbz···IPr = 102.2(2)° and DPA···IMes = 101.7(1)°.

These differences might be attributed to the differing steric profiles of IMes and **IPr** (2,4,6-trimethylphenyl, Mes *versus* 2,6-diisopropylphenyl, Dipp), though more probably these differences are due to the acidities of **DPA** ($pK_a \approx 25.0$ in DMSO)[54] *versus* Cbz ($pK_a \approx 19.9$ in DMSO).[55] Consistent with the latter hypothesis, MeOH···IMes adduct (Fig. 1a) displays a shorter hydrogen bond length (1.96(2) Å) and a more pronounced N–C–N angle of 102.5(1)° (MeOH $pK_a \sim 29.0$ in DMSO)[56,57] than the amine-based species depicted in Fig. 1a. Although making comparisons between the reactivities of different NHCs can be troublesome, relatively minor differences in the basicity of **IPr** and IMes can be assumed, for the pK_a of their parent imidazoliums' are within error (pK_a IPr·HCl = 19.29 ± 0.07, pK_a IMes·HCl = 19.40 ± 0.12).[58,59]

Though the isolation and authentication of hydrogen bonding adducts of carbenes has thus far been limited to imidazolylidene-based carbenes, hydrogen bonding adducts role in catalysis[60–63] and X–H insertion chemistry has been postulated for some time. Bertrand recently provided computational evidence for these non-traditional hydrogen bonded species as key intermediates for the reversible insertion of cyclic (alkyl)(amino)(carbene)s (CAACs) into the N–H bond of **DPA** (Fig. 1b).[34] The calculations

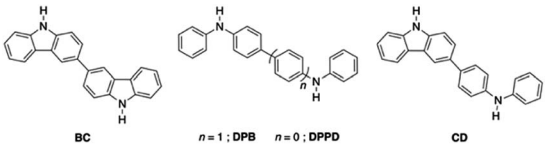

Chart 1 Ditopic secondary amines.

suggested that the process of a CAAC inserting into an N–H bond proceeds *via* non-traditional hydrogen bonded and proton transfer intermediates.

Our recent work has established that Cbz and **IPr** form a hydrogen bonding adduct (Cbz···IPr, Fig. 1a) that has a strength of association in solution (C_6D_6) of −2.8 kcal mol^{-1}.[33] Previous studies of non-traditional X–H···:C< hydrogen bonding (X = N (ref. 31) or O (ref. 32, 47, 48 and 64)) did not quantitate the strengths of interaction. Interestingly, the corresponding reaction of Cbz with CAAC from this study is reversible and yields the product of insertion of the carbene into the N–H bond of Cbz. The use of more strongly acidic N–H species with CAACs however results in proton transfer to forms salts.[33,65] Collectively, these experimental efforts help "visualize" the proposed intermediates for insertion reactions of CAACs into X–H bonds.

While these efforts have proven fruitful in identifying new species with unique hydrogen bonds, there are no steadfast rules to predict reactivity or product distribution. Crystallographic information on H···:C< hydrogen bonds shed some insight into the strength of these associations, but there are no obvious ways to correlate these metrics to solution-state measurements. Computational efforts have been made to determine the hydrogen bond basicity of carbenes, but thus far these measures have been purely theoretical.[66,67]

It is of interest therefore to gain further insights into the factors that determine when hydrogen bonding occurs in preference to proton transfer or N–H insertion for reactions between isolable carbenes and *NH*-containing molecules. An important part of this effort involves delineating the strengths of non-conventional hydrogen bonding. In order to probe this latter question in more detail, a series of symmetric and asymmetric ditopic *NH*-containing systems consisting of Cbz and **DPA** units (Chart 1; 3,3′-bicarbazole,[68] **BC**; *N*,*N*′-diphenylbenzidine, **DPB**; *N*,*N*′-diphenyl-*p*-phenylenediamine, **DPPD**, 4-(carbazol-3-yl)-*N*-phenylaniline, **CD**), which are structurally similar with differing acidities, will be reacted with a single NHC (**IPr**). These unusual platforms will allow for the gradual tuning of a single component (X–H) while having the carbene (A) remain consistent. This array of hydrogen bonded adducts will be used to assess how a NHC participates in non-traditional hydrogen bonding when presented with multiple reactive sites within single molecules.

Results and discussion

BC···2IPr adduct

Previous studies on a Cbz···IPr hydrogen bonded adduct suggested that **IPr** could form a di-hydrogen bonded adduct with **BC**, and that this adduct should be labile and display

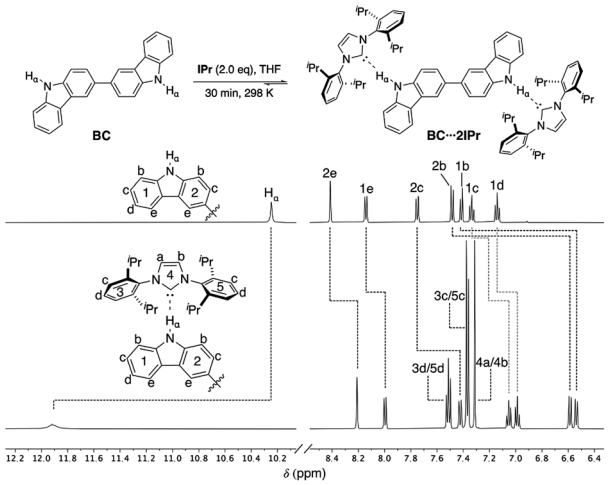

Fig. 2 Partial ^{1}H NMR spectra (500 MHz, THF-d_8) of **BC** (50 mM) and **BC**···**2IPr**. Dashed lines indicate chemical shift changes upon hydrogen bonding to **IPr**.

concentration dependent behavior. ^{1}H NMR analysis of a 1 : 2 mixture of **BC** and **IPr** in THF-d_8 reveals that significant shifts ($\Delta\delta$ > 0.05 ppm) occur for all proton resonances of the individual components, as highlighted in Fig. 2. In particular, the drastic downfield shift of H_α ($\Delta\delta \approx +1.7$ ppm) is indicative of hydrogen bonding, and is similar to the corresponding shift of H_α during formation of Cbz···IPr. The number of resonances indicate a symmetric structure for the **BC**···**2IPr** di-hydrogen bonded adduct. Consistent with this formulation, signals 1b and 2b show a substantial upfield shift ($\Delta\delta \approx -0.9$ ppm), since upon complexation they are positioned directly into the face of the Dipp groups on **IPr**. Inspection of the $^{13}C\{^1H\}$ NMR spectrum of **BC**···**2IPr** reveals a single carbenic resonance (δ 215.2 ppm) that is noticeably upfield relative to the carbenic resonance of **IPr** (δ 221.1 ppm in THF-d_8).

Vapor diffusion of hexanes into a solution of **BC**···**2IPr** in THF yielded pale yellow crystals suitable for X-ray diffraction. Crystallographic analysis of one such crystal of **BC**···**2IPr** is portrayed in Fig. 3 (see ESI† for full details). The structure confirms a two-fold hydrogen bonding adduct, with an average H1···C13 distance of 2.10 Å and a N2–C12–N3 angle of 102.2°,

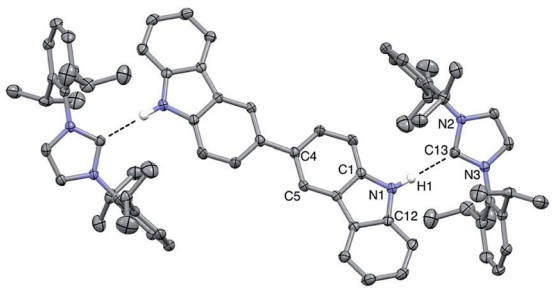

Fig. 3 ORTEP diagram (ellipsoids drawn at 50% probability) of **BC**···**2IPr**. Non-hydrogen bonding hydrogens and co-crystallized THF are omitted for clarity. Average select bond lengths (Å) and angles (°): H1···C13, 2.10; N1···C13, 2.96; N2–C13–N3, 102.2; N2–N3–C12–C1, 13.5.

which are nearly identical to corresponding parameters for the mono-functional counterpart Cbz···IPr. Interestingly, the imidazole-2-ylidene C_3N_2 and Cbz ring systems are nearly coplanar as indicated by ϕ N2–N3–C12–C1 = 13.5°, which is in line with the monotopic Cbz···IPr system (ϕ = 11.0°).

Model DPA···IPr adduct

Structural data for a DPA···IMes hydrogen bonded adduct were previously reported,[31] but for the present study related details on the corresponding **DPA**···**IPr** adduct are necessary so that closer comparisons can be made. This material was synthesized by the addition of **IPr** to a THF solution of **DPA**. Removal of solvent, followed by recrystallization from toluene at −35 °C affords pure **DPA**···**IPr** as white crystals. Hydrogen bond formation is clearly indicted in C_6D_6 by an upfield shift of the carbenic carbon resonance (218.2 ppm) compared to parent **IPr** (220.6 ppm in C_6D_6).[69] Preliminary ^{1}H NMR analysis of this material showed concentration dependent behavior. To ascertain the strength of this association a ^{1}H NMR concentration dependent study of **DPA**···**IPr** was performed in C_6D_6 over a broad concentration range (75–1 mM). Benzene is an ideal solvent in such an analysis as its impact on hydrogen bonding is minimal,[70] while also allowing for comparison to our previous measurements on Cbz···IPr (C_6D_6, concentration range of 50–1 mM).[33] This analysis revealed the association strength of **DPA**···**IPr** to be substantially weaker than Cbz···IPr ($K_d = 105 \pm 3$ M^{-1}; $\Delta G \approx -2.8$ kcal mol^{-1}), with only the *NH* resonance being significantly influenced upon complexation ($K_d = 0.85 \pm 1.05$ M^{-1} and $\Delta G \approx -0.10$ kcal mol^{-1}, see ESI† for full details).[71] This drastic preference for the more acidic amine of Cbz was also verified *via* an exchange reaction (eqn (1)):

$$\textbf{DPA}\cdots\textbf{IPr} + \text{Cbz} \rightleftharpoons \text{Cbz}\cdots\text{IPr} + \textbf{DPA} \quad (1)$$

wherein addition of Cbz to **DPA**···**IPr** results in near complete conversion to Cbz···IPr and displacement of **DPA**. The dynamic (on the NMR timescale) nature of the mixture is indicated by the fact that a single hydrogen bonding *NH* resonance is observed (albeit not to the extent of the pure adducts, see ESI†) for each of the reaction pairs (**DPA**···**IPr**/**DPA** and Cbz···IPr/Cbz).

Ditopic DPB···2IPr and DPPD···2IPr adducts

Both ditopic **DPB** and **DPPD** yield 1 : 2 adducts **DPB**···**2IPr** and **DPPD**···**2IPr**, respectively, upon reaction with two equivalents of **IPr** (Fig. 4, top) in THF. As previously observed, **DPB**···**2IPr** and **DPPD**···**2IPr** are in equilibrium with their individual components, and at higher NMR concentrations these solutions exist predominately as the di-hydrogen bonded species. ^{1}H NMR analyses (**DPB**···**2IPr**, **DPPD**···**2IPr**), as shown in Fig. 4, highlights the subtle chemical shift changes ($\Delta\delta$ < 0.20 ppm) for resonances compared to **BC**···**2IPr** ($\Delta\delta$ > 0.15 ppm). Though these shifts in proton resonances are smaller, the overall directionality matches that observed for **BC**···**2IPr**. This is best realized in the *NH* signal, H_β, which shifts by $\Delta\delta$ = 0.20 ppm (**DPB**···**2IPr**) and $\Delta\delta$ = 0.15 ppm (**DPPD**···**2IPr**), indicative of a significantly weaker hydrogen bond.

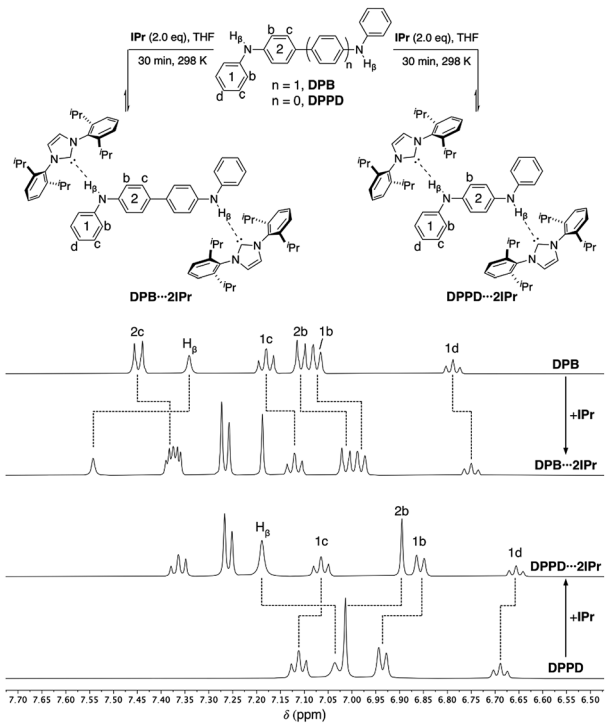

Fig. 4 Partial ^{1}H NMR spectra (500 MHz, THF-d_8) of **DPB** (50 mM), **DPB**···**2IPr**, **DPPD**···**2IPr**, and **DPPD** (50 mM). Dashed lines highlight the chemical shift changes upon hydrogen bonding to **IPr**.

Crystals of **DPPD**···**2IPr** suitable for a X-ray diffraction studies were obtained by chilling a solution of **DPPD**···**2IPr** in a 3 : 2 hexanes : THF solvent mixture at −35 °C for several days. The resulting solid-state structure of **DPPD**···**2IPr** is portrayed in Fig. 5. The H1···C24 distance of 2.30(2) Å matches that found for the DPA···IMes adduct, as is the interior N2–C13–N3 angle of 101.9(1)°. The dihedral between the pseudo-planes of **DPPD**···**2IPr** (ϕ N2–N3–C2–C4 = 17°) are in agreement with **BC**···**2IPr**, and slightly less pronounced than DPA···IMes (ϕ = 38°). The N1–H1···C24 bond angle is nearly linear (171°), albeit quite bent relative to DPA···IMes (N–H···:C$\swarrow$ = 179°). The hydrogen bond distances are within the sum of the van der Waal radii, and display closer contacts than the hydrogen bond

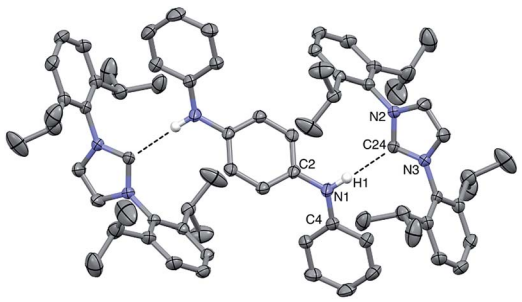

Fig. 5 ORTEP diagram (ellipsoids drawn at 50% probability) of **DPPD**···**2IPr**. Non-hydrogen bonding hydrogens are omitted for clarity. Select bond lengths (Å) and angles (°): H1···C24, 2.30(2); N1···C24, 3.174(2); N2–C13–N3, 101.9(1); N2–N3–C4–C2, −17.41(7).

adducts of the Ong group, where carbenes with pendant secondary amines form dimers in the solid-state.[44,45] By contrast, all attempts to crystallize **DPB**···**2IPr** resulted in dissociation of the adduct into individual components. It appears that the poor solubility of **DPB** leads to preferential precipitation/crystallization of **DPB**, which is in facile equilibrium with **IPr** and **DPB**···**2IPr** (*vide infra*).

Analysis of the metric data obtained for the symmetric ditopic *NH*-bearing adducts in both solid- and solution-state reveals several interesting insights. In the solid-state the N–C–N angles within **IPr** (101.5°)[69] relax upon formation of hydrogen bonded species **DPPD**···**2IPr** (101.9°) and **BC**···**2IPr** (102.2°). A greater distortion of the N–C–N angle is thus associate with greater interaction, and if taken to an extreme would result in proton transfer (where imidazolium salts typically feature N–C–N angles of ∼108°).[30] The length of the hydrogen bonds (H···:C$\swarrow$ distance; **DPPD**···**2IPr**, 2.30 Å; **BC**···**2IPr**, 2.10 Å) also correlate well with the presumed strength of association based on measurements on the monofunctional amine counterparts (*vide supra*).

While ^{1}H NMR spectra show that the changes in the chemical shifts for protons involved in hydrogen bonding can be predictive of association strengths, the shifts observed in the ^{13}C{^{1}H} NMR spectra for the carbenic carbon are also quite sensitive to these external interactions. As the strength of the hydrogen bond increases the carbenic carbon shifts upfield.[30]

Specifically, the ^{13}C{^{1}H} NMR spectra of **BC**···**2IPr** (215.2 ppm) shows a greater $\Delta\delta$ (free **IPr** δ 221.1 ppm) than either **DPB**···**2IPr** (δ 220.1 ppm) and **DPPD**···**2IPr** (δ 220.3 ppm). ^{13}C spectroscopy might thus serve as a new tool for assessing the strength of the hydrogen bond in non-traditional systems, adding to other experimental measures used to assess the properties of carbenes as ligands (*i.e.* measuring π-acidity *via* ^{31}P or ^{77}Se NMR spectroscopy[72] and carbene-metal ligand strength assessed *via* ^{13}C spectroscopy[73]).

Internal competitive hydrogen bonding

To probe the competitive nature of these hydrogen bonding adducts mixed carbazole-diphenylamine species **CD** was synthesized *via* Suzuki–Miyaura cross-coupling in modest yield (55% isolated, see ESI† for details). Reactions of **CD** with one and two equivalents of **IPr** were thus examined (Fig. 6, upper). As expected, formation of the mono- and di-carbene adducts **CD**···**IPr** and **CD**···**2IPr** is observable by NMR spectroscopy at elevated concentrations. Fig. 6 compares partial ^{1}H NMR spectra of these products contrasted against **CD**, highlighting the proton resonances impacted by NHC association. In alignment with the findings above, preferential interaction of the NHC occurs with the carbazole unit of **CD** upon addition of one equivalent of **IPr** (black dotted lines in Fig. 6). This assessment is confirmed by the signals for carbazole fragment of **CD** shifting in the same fashion as the symmetric **BC**···**2IPr**, with the caveat that shifts are only ∼65% the overall $\Delta\delta$ of their symmetric counterpart. This may reflect the fact that **IPr** equilibrates between both carbazole and diphenylamine *NH* residues to some extent. The perturbations of the proton

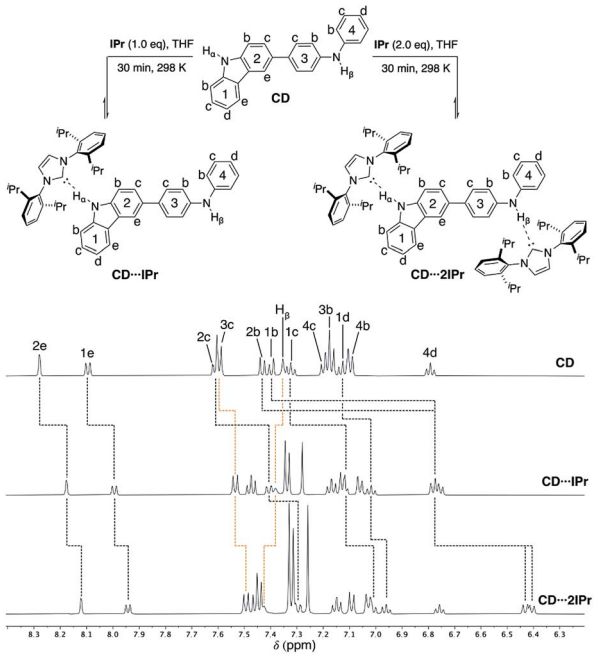

Fig. 6 Partial ^{1}H NMR spectra (500 MHz, THF-d_8) of **CD** (50 mM), **CD**···**IPr**, and **CD**···**2IPr**, highlighting the chemical shift changes upon hydrogen bonding to **IPr**. **CD** H_α (10.25 ppm), **CD**···**IPr** H_α (11.30 ppm), and **CD**···**2IPr** H_α (12.40 ppm) are broadened due to exchange, see ESI† (rings 1 and 2 = black dotted lines, rings 3 and 4 = orange dotted lines).

resonances on rings 3 and 4 (orange dotted lines) are reminiscent of **DPB**···**2IPr** and **DPPD**···**2IPr**, albeit only minor in comparison to rings 1 and 2.

Upon addition of two equivalents of **IPr** to **CD**, the ^{1}H NMR chemical shifts of **CD**···**2IPr** are a near match to the symmetric diamine counterparts, **BC**···**2IPr** and **DPB**···**2IPr** respectively. The realignment of the ^{1}H spectra to mirror the symmetric analogues confirms formation of **CD**···**2IPr**. Due to the rapid exchange of **IPr** between both *NH* sites on **CD** the $^{13}C\{^{1}H\}$ NMR spectra yield a singular shift for the carbenic resonance. The observed shifts for asymmetric **CD**···**2IPr** (δ 217.4 ppm) and **CD**···**IPr** (δ 216.4 ppm) fall between their respective symmetric counterparts (**BC**···**2IPr**, δ 215.2 ppm, **DPB**···**2IPr**, δ 220.1 ppm). Unsurprisingly the $^{13}C\{^{1}H\}$ NMR signal in **CD**···**IPr** resides closer to **BC**···**2IPr**, verifying our ^{1}H measurements which show that **IPr** preferentially binds to the carbazole side of the ditopic system. When both *NH* sites are satisfied in **CD**···**2IPr** the carbenic carbon resonance is a near perfect average of the observed resonances for the symmetric species (**BC**···**2IPr** and **DPB**···**2IPr** average resonance carbenic resonance $\approx$ 217.6 ppm).

Unfortunately attempts to obtain single crystals of either **CD**···**IPr** and **CD**···**2IPr** were thwarted by the preferential crystallization of **CD** from solutions of these materials (see ESI† for crystallographic details). While this may be due to the reduced solubility of **CD** relative to **IPr**, the probable cause is the labile nature of the N–H···:C< bond not being conducive to solid-state analysis.

Table 1 Summation of solid- and solution-state metrics[a]

	N–C–N (°)	^{13}C δ (ppm)	^{1}H $\Delta\delta$ (ppm)	pK_a
IPr	101.5[b]	221.1	—	19.3[c]
BC···**2IPr**	102.2	215.2	1.66	19.9
DPB···**2IPr**	—	220.1	0.20	25.0
DPPD···**2IPr**	101.9	220.3	0.15	25.0
CD···**2IPr**	—	217.4	0.99[d]	22.5[d]

[a] ^{1}H $\Delta\delta$ is calculated relative to each adducts parent species at 50 mM in THF-d_8. [b] See ref. 69. [c] pK_a of the conjugate acid (**IPr**·HCl).[58,59] [d] Average values.

Conclusion

Through a series of symmetric and asymmetric ditopic secondary amines the strength of a X–H···:C< hydrogen bond can be directly assessed *via* several solid- and solution-state factors, summarized in Table 1. Paramount in predicting the strength of the association is the pK_a of the parent X–H species, which in these examples correlates well with both solid- and solution-state metrics. In the solid-state limiting the degrees of freedom in the parent molecule is vital, wherein systems with even weak hydrogen bonds can be crystallized in their adduct form (DPPD···2IPr). In BC, DPB, and DPPD systems solution-state analysis is simplified due their high degree of symmetry and rapid equilibrium of the N–H···**IPr** interaction. In each of these species both the $\Delta\delta$ of the proton participating in hydrogen bonding and the ^{13}C resonance of the carbenic carbon are indicators of hydrogen bond strength. ^{1}H NMR spectra show that upon hydrogen bonding with **IPr** the monomers are rigidified, with proton resonances far removed from area of interaction changing significantly in comparison to the unhindered molecules. When starving the asymmetric **CD** system of **IPr**, the carbene primarily interacts with the more acidic carbazole residue as evidenced by both ^{1}H and ^{13}C spectroscopy. When enough **IPr** is supplied to satisfy both *NH* sites the carbenic carbon resonance falls directly between the symmetric ^{13}C residues, indicating a system that is in rapid equilibrium on the NMR timescale. The reversible nature of these systems and the ability to predict hydrogen bond strength through both solid- and solution-state metrics could lead to further developments in systems chemistry. Efforts to explore higher functionality *NH*-containing systems and carbenes are currently underway.

Conflicts of interest

The authors declare no conflicts of interest.

Acknowledgements

We thank the National Science Foundation (CHE-1464855 and CHE-1955845) for their support of this work.

Notes and references

1 G. A. Jeffrey and W. Saenger, *Hydrogen Bonding in Biological Systems*, Springer, Berlin, 1991.

2 L. McFail-Isom, C. C. Sines and L. D. Williams, DNA Structure: Cations in Charge?, *Curr. Opin. Struct. Biol.*, 1999, **9**, 298–304.
3 J. A. Subirana and M. Soler-López, Cations as Hydrogen Bond Donors: A View of Electrostatic Interactions in DNA, *Annu. Rev. Biophys. Biomol. Struct.*, 2003, **32**, 27–45.
4 D. Meyer, P. Neumann, R. Ficner and K. Tittmann, Observation of a Stable Carbene at the Active Site of a Thiamin Enzyme, *Nat. Chem. Biol.*, 2013, **9**, 488–490.
5 A. G. Doyle and E. N. Jacobsen, Small-Molecule H-Bond Donors in Asymmetric Catalysis, *Chem. Rev.*, 2007, **107**, 5713–5743.
6 P. Gallo, K. Amann-Winkel, C. A. Angell, M. A. Anisimov, F. Caupin, C. Chakravarty, E. Lascaris, T. Loerting, A. Z. Panagiotopoulos, J. Russo, J. A. Sellberg, H. E. Stanley, H. Tanaka, C. Vega, L. Xu and L. G. M. Pettersson, Water: A Tale of Two Liquids, *Chem. Rev.*, 2016, **116**, 7463–7500.
7 F. Cipcigan, V. Sokhan, G. Martyna and J. Crain, Structure and Hydrogen Bonding at the Limits of Liquid Water Stability, *Sci. Rep.*, 2018, **8**, 1–8.
8 S. H. Gellman, Foldamers: A Manifesto, *Acc. Chem. Res.*, 1998, **31**, 173–180.
9 D. Núñez-Villanueva, G. Iadevaia, A. E. Stross, M. A. Jinks, J. A. Swain and C. A. Hunter, H-Bond Self-Assembly: Folding versus Duplex Formation, *J. Am. Chem. Soc.*, 2017, **139**, 6654–6662.
10 H. Szatyłowicz, Structural Aspects of the Intermolecular Hydrogen Bond Strength: H-Bonded Complexes of Aniline, Phenol and Pyridine Derivatives, *J. Phys. Org. Chem.*, 2008, **21**, 897–914.
11 S. J. Pike, E. Lavagnini, L. M. Varley, J. L. Cook and C. A. Hunter, H-Bond Donor Parameters for Cations, *Chem. Sci.*, 2019, **10**, 5943–5951.
12 M. D. Joesten, Hydrogen Bonding and Proton Transfer, *J. Chem. Educ.*, 1982, **59**, 362–366.
13 J. Emsley, Very Strong Hydrogen Bonding, *Chem. Soc. Rev.*, 1968, **9**, 91–124.
14 R. H. Crabtree, Hypervalency Secondary Bonding and Hydrogen Bonding: Siblings under the Skin, *Chem. Soc. Rev.*, 2017, **46**, 1720–1729.
15 G. R. Desiraju and T. Steiner, *The Weak Hydrogen Bond: In Structural Chemistry and Biology*, 2001.
16 J. A. Platts, S. T. Howard and K. Woźniak, Quantum Chemical Evidence for C–H···C Hydrogen Bonding, *Chem. Commun.*, 1996, **1**, 63–64.
17 A. S. Batsanov, M. G. Davidson, J. A. K. Howard, S. Lamb and C. Lustig, Phosphonium Ylides as Hydrogen Bond Acceptors: Inter Molecular C–H···C Interactions in the Crystal Structure of Triphenylphosphonium Benzylide, *Chem. Commun.*, 1996, **15**, 1791–1792.
18 A. J. Arduengo, R. L. Harlow and M. Kline, A Stable Crystalline Carbene, *J. Am. Chem. Soc.*, 1991, **113**, 361–363.
19 M. N. Hopkinson, C. Richter, M. Schedler and F. Glorius, An Overview of *N*-Heterocyclic Carbenes, *Nature*, 2014, **510**, 485–496.
20 J. Chen and Y. Huang, Asymmetric Catalysis with *N*-Heterocyclic Carbenes as Non-Covalent Chiral Templates, *Nat. Commun.*, 2014, **5**, 1–8.
21 V. Nesterov, D. Reiter, P. Bag, P. Frisch, R. Holzner, A. Porzelt and S. Inoue, NHCs in Main Group Chemistry, *Chem. Rev.*, 2018, **118**, 9678–9842.
22 E. Peris, Smart *N*-Heterocyclic Carbene Ligands in Catalysis, *Chem. Rev.*, 2018, **118**, 9988–10031.
23 M. Soleilhavoup and G. Bertrand, Cyclic (Alkyl)(Amino) Carbenes (CAACs): Stable Carbenes on the Rise, *Acc. Chem. Res.*, 2015, **48**, 256–266.
24 M. Melaimi, R. Jazzar, M. Soleilhavoup and G. Bertrand, Cyclic (Alkyl)(Amino)Carbenes (CAACs): Recent Developments, *Angew. Chem., Int. Ed.*, 2017, **56**, 10046–10068.
25 A. J. Arduengo, Looking for Stable Carbenes: The Difficulty in Starting Anew, *Acc. Chem. Res.*, 1999, **32**, 913–921.
26 R. Visbal and M. C. Gimeno, *N*-Heterocyclic Carbene Metal Complexes: Photoluminescence and Applications, *Chem. Soc. Rev.*, 2014, **43**, 3551–3574.
27 A. Doddi, M. Peters and M. Tamm, *N*-Heterocyclic Carbene Adducts of Main Group Elements and Their Use as Ligands in Transition Metal Chemistry, *Chem. Rev.*, 2019, **119**, 6994–7112.
28 I. Alkorta, I. Rozas and J. Elguero, Non-Conventional Hydrogen Bonds, *Chem. Soc. Rev.*, 1998, **27**, 163–170.
29 J. K. W. Chui, T. Ramnial and J. A. C. Clyburne, N-Heterocyclic Carbenes: Exotic Molecules as Precursors to Unusual Hydrogen Bonds, *Comments Inorg. Chem.*, 2003, **24**, 165–187.
30 A. J. I. Arduengo, S. F. Gamper, M. Tamm, J. C. Calabrese, F. Davidson and H. A. Craig, A Bis(Carbene)—Proton Complex: Structure of a C—H—C Hydrogen Bond, *J. Am. Chem. Soc.*, 1995, **117**, 572–573.
31 J. A. Cowan, J. A. C. Clyburne, M. G. Davidson, R. L. W. Harris, J. A. K. Howard, P. Küpper, M. A. Leech and S. P. Richards, On the Interaction between *N*-Heterocyclic Carbenes and Organic Acids: Structural Authentication of the First N—H···C Hydrogen Bond and Remarkably Short C—H···O Interactions, *Angew. Chem., Int. Ed.*, 2002, **41**, 1432–1434.
32 M. Movassaghi and M. A. Schmidt, *N*-Heterocyclic Carbene-Catalyzed Amidation of Unactivated Esters with Amino Alcohols, *Org. Lett.*, 2005, **7**, 2453–2456.
33 J. M. Kieser, Z. J. Kinney, J. R. Gaffen, S. Evariste, A. M. Harrison, A. L. Rheingold and J. D. Protasiewicz, Three Ways Isolable Carbenes Can Modulate Emission of NH-Containing Fluorophores, *J. Am. Chem. Soc.*, 2019, **141**, 12055–12063.
34 D. Tolentino, S. Neale, C. Isaac, S. A. Macgregor, M. K. Whittlesey, R. Jazzar and G. Bertrand, Reductive Elimination at Carbon under Steric Control, *J. Am. Chem. Soc.*, 2019, **141**, 9823–9826.
35 I. Alkorta and J. Elguero, Carbenes and Silylenes as Hydrogen Bond Acceptors, *J. Phys. Chem.*, 1996, **100**, 19367–19370.

36 A. M. Magill, K. J. Cavell and B. F. Yates, Basicity of Nucleophilic Carbenes in Aqueous and Nonaqueous Solvents—Theoretical Predictions, *J. Am. Chem. Soc.*, 2004, **126**, 8717–8724.

37 J.-L. Mieusset and U. H. Brinker, The Carbene Reactivity Surface: A Classification, *J. Org. Chem.*, 2008, **73**, 1553–1558.

38 O. Hollóczki, Unveiling the Peculiar Hydrogen Bonding Behavior of Solvated *N*-Heterocyclic Carbenes, *Phys. Chem. Chem. Phys.*, 2016, **18**, 126–140.

39 J. E. Del Bene, I. Alkorta and J. Elguero, Hydrogen-Bonded Complexes with Carbenes as Electron-Pair Donors, *Chem. Phys. Lett.*, 2017, **675**, 46–50.

40 L. A. Leites, G. I. Magdanurov, S. S. Bukalov and R. West, Intermolecular =C–H···:C Hydrogen Bond in a Crystalline Unsaturated Arduengo-Type Carbene, *Mendeleev Commun.*, 2008, **18**, 14–15.

41 M. Kapitein, M. Balmer and C. von Hanisch, A Sterically Encumbered 13/15 Cycle and Its Cleavage with *N*-Heterocyclic Carbenes and Other Lewis Bases, *Z. Anorg. Allg. Chem.*, 2016, **642**, 1275–1281.

42 P. A. Petrov, T. S. Sukhikh and M. N. Sokolov, NHC Adducts of Tantalum Amidohalides: The First Example of NHC Abnormally Coordinated to an Early Transition Metal, *Dalton Trans.*, 2017, **46**, 4902–4906.

43 H. Jong, B. O. Patrick and M. D. Fryzuk, Amine-Tethered N-Heterocyclic Carbene Complexes of Rhodium(I), *Can. J. Chem.*, 2008, **86**, 803–810.

44 W. C. Shih, C. H. Wang, Y. T. Chang, G. P. A. Yap and T. G. Ong, Synthesis and Structure of an Amino-Linked *N*-Heterocyclic Carbene and the Reactivity of Its Aluminum Adduct, *Organometallics*, 2009, **28**, 1060–1067.

45 C.-Y. Y. Li, Y.-Y. Y. Kuo, J.-H. H. Tsai, G. P. A. A. Yap and T.-G. G. Ong, Amine-Linked *N*-Heterocyclic Carbenes: The Importance of an Pendant Free-Amine Auxiliary in Assisting the Catalytic Reaction, *Chem.–Asian J.*, 2011, **6**, 1520–1524.

46 H. Braunschweig, W. C. Ewing, K. Geetharani and M. Schäfer, The Reactivities of Iminoboranes with Carbenes: BN Isosteres of Carbene-Alkyne Adducts, *Angew. Chem., Int. Ed.*, 2015, **54**, 1662–1665.

47 M. A. Schmidt, P. Müller and M. Movassaghi, On the Interactions of *N,N′*-Bismesitylimidazolin-2-Yl and Alcohols, *Tetrahedron Lett.*, 2008, **49**, 4316–4318.

48 N. A. Giffin, M. Makramalla, A. D. Hendsbee, K. N. Robertson, C. Sherren, C. C. Pye, J. D. Masuda and J. A. C. Clyburne, Anhydrous TEMPO-H: Reactions of a Good Hydrogen Atom Donor with Low-Valent Carbon Centres, *Org. Biomol. Chem.*, 2011, **9**, 3672–3680.

49 A. H. Raut, G. Karir and K. S. Viswanathan, Matrix Isolation Infrared and Ab Initio Study of the Interaction of *N*-Heterocyclic Carbene with Water and Methanol: A Case Study of a Strong Hydrogen Bond, *J. Phys. Chem. A*, 2016, **120**, 9390–9400.

50 R. Srivastava, R. Moneuse, J. Petit, P. A. Pavard, V. Dardun, M. Rivat, P. Schiltz, M. Solari, E. Jeanneau, L. Veyre, C. Thieuleux, E. A. Quadrelli and C. Camp, Early/Late Heterobimetallic Tantalum/Rhodium Species Assembled Through a Novel Bifunctional NHC-OH Ligand, *Chem.–Eur. J.*, 2018, **24**, 4361–4370.

51 B. Maji, M. Breugst and H. Mayr, *N*-Heterocyclic Carbenes: Organocatalysts with Moderate Nucleophilicity but Extraordinarily High Lewis Basicity, *Angew. Chem., Int. Ed.*, 2011, **50**, 6915–6919.

52 A. Levens, F. An, M. Breugst, H. Mayr and D. W. Lupton, Influence of the *N*-Substituents on the Nucleophilicity and Lewis Basicity of *N*-Heterocyclic Carbenes, *Org. Lett.*, 2016, **18**, 3566–3569.

53 T. Steiner, The Hydrogen Bond in the Solid State, *Angew. Chem., Int. Ed.*, 2002, **41**, 48–76.

54 F. G. Bordwell, J. C. Branca, D. L. Hughes and W. N. Olmstead, Equilibriums Involving Organic Anions in Dimethyl Sulfoxide and *N*-Methylpyrrolidin-2-One: Acidities, Ion Pairing, and Hydrogen Bonding, *J. Org. Chem.*, 1980, **45**, 3305–3313.

55 F. G. Bordwell, G. E. Drucker and H. E. Fried, Acidities of Carbon and Nitrogen Acids: The Aromaticity of the Cyclopentadienyl Anion, *J. Org. Chem.*, 1981, **46**, 632–635.

56 P. Ballinger and F. A. Long, Acid Ionization Constants of Alcohols. II. Acidities of Some Substituted Methanols and Related Compounds, *J. Am. Chem. Soc.*, 1960, **82**, 795–798.

57 W. N. Olmstead, Z. Margolin and F. G. Bordwell, Acidities of Water and Simple Alcohols in Dimethyl Sulfoxide Solution, *J. Org. Chem.*, 1980, **45**, 3295–3299.

58 M. H. Dunn, N. Konstandaras, M. L. Cole and J. B. Harper, Targeted and Systematic Approach to the Study of pKa Values of Imidazolium Salts in Dimethyl Sulfoxide, *J. Org. Chem.*, 2017, **82**, 7324–7331.

59 Z. Wang, X. S. Xue, Y. Fu and P. Ji, Comprehensive Basicity Scales for *N*-Heterocyclic Carbenes in DMSO: Implications on the Stabilities of *N*-Heterocyclic Carbene and CO_2 Adducts, *Chem.–Asian J.*, 2020, **15**, 169–181.

60 S. Santra, A. Porey, B. Jana and J. Guin, *N*-Heterocyclic Carbenes as Chiral Brønsted Base Catalysts: A Highly Diastereo- and Enantioselective 1,6-Addition Reaction, *Chem. Sci.*, 2018, **9**, 6446–6450.

61 S. Gehrke and O. Hollóczki, Hydrogen Bonding of *N*-Heterocyclic Carbenes in Solution: Mechanisms of Solvent Reorganization, *Chem.–Eur. J.*, 2018, **24**, 11594–11604.

62 O. Hollóczki, The Mechanism of *N*-Heterocyclic Carbene Organocatalysis through a Magnifying Glass, *Chem.–Eur. J.*, 2020, **26**, 4885–4894.

63 S. Santra, U. Maji and J. Guin, Enantioselective α-Amination of Acyclic 1,3-Dicarbonyls Catalyzed by *N*-Heterocyclic Carbene, *Org. Lett.*, 2020, **22**, 468–473.

64 R. Guo, X. Huang, M. Zhao, Y. Lei, Z. Ke and L. Kong, Bifurcated Hydrogen-Bond-Stabilized Boron Analogues of Carboxylic Acids, *Inorg. Chem.*, 2019, **58**, 13370–13375.

65 C. Pi, X. Yu and W. Zheng, Imidazolium 1,3-Benzazaphospholide Ion Pairs with Strong C–H···N Hydrogen Bonds — Synthesis, Structures, and Reactivity, *Eur. J. Inorg. Chem.*, 2015, **2015**, 1804–1810.

66 J. A. Platts, Theoretical Prediction of Hydrogen Bond Donor Capacity, *Phys. Chem. Chem. Phys.*, 2000, **2**, 973–980.

67 M. H. Abraham, J. Elguero and I. Alkorta, The Hydrogen-Bond Basicity of Carbenes, *Croat. Chem. Acta*, 2018, **91**, 121–124.

68 S. Mallick, S. Maddala, K. Kollimalayan and P. Venkatakrishnan, Oxidative Coupling of Carbazoles: A Substituent-Governed Regioselectivity Profile, *J. Org. Chem.*, 2019, **84**, 73–93.

69 A. J. Arduengo, H. A. Craig, J. R. Goerlich, W. J. Marshall and M. Unverzagt, Imidazolylidenes, Imidazolinylidenes and Imidazolidines, *Tetrahedron*, 1999, **55**, 14523–14534.

70 J. L. Cook, C. A. Hunter, C. M. R. Low, A. Perez-Velasco and J. G. Vinter, Solvent Effects on Hydrogen Bonding, *Angew. Chem., Int. Ed.*, 2007, **46**, 3706–3709.

71 M. Chu, A. N. Scioneaux and C. S. Hartley, Solution-Phase Dimerization of an Oblong Shape-Persistent Macrocycle, *J. Org. Chem.*, 2014, **79**, 9009–9017.

72 D. Munz, Pushing Electrons — Which Carbene Ligand for Which Application?, *Organometallics*, 2018, **37**, 275–289.

73 D. Tapu, D. A. Dixon and C. Roe, ^{13}C NMR Spectroscopy of "Arduengo-Type" Carbenes and Their Derivatives, *Chem. Rev.*, 2009, **109**, 3385–3407.